Journal of Power Sources 237 (2013) 84–97

Contents lists available at SciVerse ScienceDirect

Journal of Power Sources

journal homepage: www.elsevier.com/locate/jpowsour

Review

Cathode-supported tubular solid oxide fuel cell technology: A critical review

Kevin Huang [a,*], Subhash C. Singhal [b]

[a] SmartState Center of Solid Oxide Fuel Cells, Department of Mechanical Engineering, University of South Carolina, Columbia, SC 29201, USA
[b] Pacific Northwest National Laboratory, Richland, WA 99352, USA

HIGHLIGHTS

- A broad overview of cathode-supported tubular solid oxide fuel cell technology.
- Highlights of the 50-year's accomplishments achieved by Siemens/Westinghouse engineers.
- Inclusion of a large amount of technical information unpublished before.
- An essential document summarizing one of the most important solid oxide fuel cell technologies.

ARTICLE INFO

Article history:
Received 9 January 2013
Received in revised form
26 February 2013
Accepted 1 March 2013
Available online 28 March 2013

Keywords:
Solid oxide fuel cells
Power generation
Cathode
Tubular
Electrical performance

ABSTRACT

Over the past half-century, Siemens/Westinghouse systematically developed the cathode-supported tubular solid oxide fuel cell (SOFC) technology and demonstrated the world's first highly efficient, longest running 100-kWe class solid oxide fuel cell/combined heat and power (SOFC/CHP) system and the first highest-efficiency, 220-kWe class pressurized SOFC/gas turbine (PSOFC/GT) hybrid system based on this technology. This review provides a broad overview on this technology from the perspectives of materials, manufacturing, cell design, system integration and electrical testing. It starts from the basic facts of a SOFC, where the working principle, advantages, types and applications of SOFCs are discussed. It then focuses on cathode-supported tubular SOFCs, one important type of SOFC design, by providing detailed technical information on engineering innovations, materials advances, manufacturing processes and electrical performance of Siemens/Westinghouse's cylindrical and flattened ribbed tubular cells. The review concludes with a high-level summary of the SOFC systems manufactured and demonstrated by Siemens/Westinghouse in the past few decades.

1. Introduction

1.1. Basic facts of solid oxide fuel cells

Fossil fuels are the primary energy source currently powering human society, and will be probably so for the next several decades. Converting the resource-limited fossil fuels into useful forms of energy in the most efficient manner with minimal environmental impact has become the theme for the development of modern energy technology and making of the energy policy. High-temperature solid oxide fuel cells (SOFCs) emerge as the leader in chemical-to-electrical conversion efficiency, fuel flexibility and environmental impact amongst all types of power generation systems [1–5]. They represent the next-generation energy technology poised to offer clean and efficient power generation to the future global energy infrastructure. The compactness, modularity, and durability of high-temperature SOFCs allow particular applications in stationary, distributed power generation, a niche market in which conventional internal combustion engines (ICEs) find it difficult to compete [6–8]. It is these unique advantages of SOFCs that have attracted lasting interest in research and commercialization of SOFCs worldwide over the last several decades.

1.1.1. Working principle and functional components

Similar to any batteries of our daily use, an SOFC produces electricity from the chemical energy in fuels through three basic functional elements, namely electrolyte, cathode, and anode; electron-conducting interconnect and cell-to-cell connector are needed for connecting single cells into multi-cell bundles/stacks [1–3]. The materials for these components are either ceramics or metals. The functionality of an electrolyte is to transport oxygen continuously and solely in the form of O^{2-} from cathode to anode under a gradient of electrochemical potential of oxygen. To enable O^{2-} ion migration across the electrolyte, the cathode, which is

* Corresponding author.
E-mail addresses: kevin.huang@sc.edu (K. Huang), singhal@pnnl.gov (S.C. Singhal).

0378-7753/$ – see front matter © 2013 Elsevier B.V. All rights reserved.
http://dx.doi.org/10.1016/j.jpowsour.2013.03.001

supplied with oxygen, has to convert O_2 into O^{2-}, a process known as oxygen reduction reaction (ORR). Similarly, the anode of fuel supply accepts O^{2-} delivered by the electrolyte and converts it into H_2O, CO_2 and electrons by oxidizing hydrogen or hydrocarbon fuels, a process known as fuel oxidation reaction (FOR). The electrons required for the ORR are released by the FOR and arrive at the cathode via an external circuitry, by which the production of electricity is realized. Fig. 1 illustrates a schematic of the working principle of a SOFC. The overall driving force for a SOFC is the gradient of electrochemical potential of oxygen existing between a cathode of high partial pressure of oxygen and an anode of low partial pressure of oxygen.

The maximum cell voltage of a typical single SOFC with air as an oxidant is about 1.2 V, depending on temperature, system pressure and fuel composition. This level of voltage is inadequate for any type of practical application. To build up a sufficiently high voltage and power, multiple single cells have to be connected in series and/or parallel in an array with the aid of interconnects and/or cell-to-cell connectors. Like a battery, each SOFC component presents an internal resistance to either electronic or ionic current flow, causing voltage loss. The terminal cell voltage is, therefore, the Open Circuit Voltage (or Electromotive Force, EMF, if no fuel loss is caused by any means) reduced by the individual voltage loss of each cell component.

One radical requirement for an operational SOFC is to realize oxygen transport across the electrolyte in the form of pure O^{2-}, but not in the form of O_2. To achieve this, dense barriers separating air and fuel have to be established. For the one-end-closed cathode-supported tubular SOFC design, such barriers are achieved by the electrolyte and interconnect in a unique geometry, only allowing air and fuel to meet at the open-end, where combustion occurs after the fuel is mostly utilized over the exposed cylindrical outer surface [8]; no physical gas seals are needed. In contrast, for the planar SOFC design, gas seals have to be applied along the perimeters of interconnect/electrodes and electrolyte/electrodes in order to prevent air from mixing with fuel; this often presents a challenge to the reliability and stability of planar SOFCs over a prolonged operation [9–13].

1.1.2. Advantages of SOFCs

The fuel cell is a device that directly converts the chemical energy in fuels into electrical power in an electrochemical manner [1–3]. Therefore, it is not limited by the Carnot Cycle, and has an inherently higher electrical efficiency than conventional ICEs, particularly for the less than MW class. Higher electrical efficiency infers a reduced CO_2 emission per unit electricity produced if hydrocarbons are used as fuels, which has become increasingly important as we endeavor to minimize the carbon emissions from fossil fuel based power generation. Another conceivable benefit is the benign environmental impact from a fuel cell generator over an ICE. Due to its relatively low operating temperature, the formation and therefore the emission of nitrogen oxides (collectively known as NO_x) are negligible. Use of a desulfurizer subsystem in a fuel cell generator ensures almost zero emission of sulfur oxides (collectively known as SO_x). In addition, fuel cell power generators are much quieter, less vibrating and incur less maintenance costs than a conventional ICE during operation, and therefore they offer a competitive application in distributed as well as premium stationary power generation.

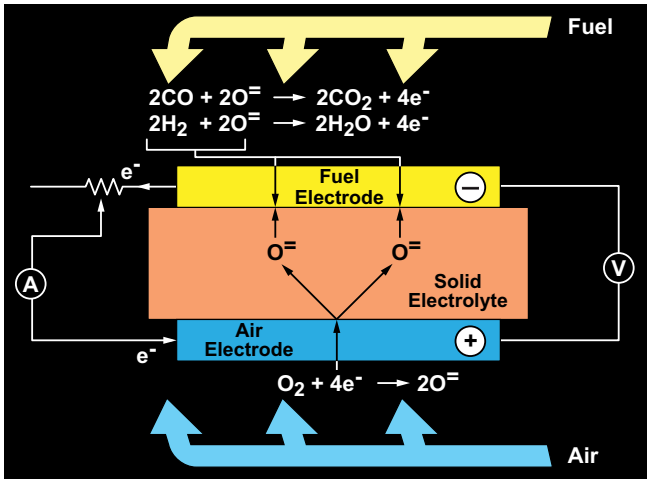

Fig. 1. A schematic illustration of the working principle of SOFCs.

For SOFCs operating at higher temperatures, there are added advantages. High temperature operation, typically in the range of 600–1000 °C, not only provides high quality waste heat, but also effectively activates the processes of reforming and electrochemical oxidation of hydrocarbon fuels in the presence of catalysts [14,15]. This advantage is technically important for several reasons. First, it enables SOFCs to use most hydrocarbon fuels, either in the gaseous or liquid state, provided that they are properly cleaned and reformed into simple fuels such as H_2 and CO [14,15]. This is in contrast to low temperature fuel cells such as PEM fuel cells where CO poisons the anode [16,17]. Second, excessive heat produced from the electrochemical oxidation of fuels can be utilized by the highly endothermic steam reforming reaction simultaneously occurring, which makes internal on-cell reformation possible [18]. Such integration further increases the overall system efficiency. Co-production of heat and power, often known as Combined Heat and Power (CHP), is the third added advantage of high-temperature SOFCs [19]. The recovery of waste heat along with the production of electricity pushes the total energy efficiency of such a system to be in the range of 85–90%. Another way of recovering waste heat is to combine a micro gas turbine with a SOFC stack to form a hybrid system [19–22]. To maximize the electrical efficiency, the SOFC/micro gas turbine hybrid is often operated under pressure that can boost both the performance of the SOFC stack and the effectiveness of the micro gas turbine. To be even more efficient, a bottoming cycle steam turbine can be added into the above hybrid system [19,20]. This is particularly preferable for over 100-MWe size generators. The hybrid SOFC generator system has been demonstrated in a 220-kWe class by Siemens/Westinghouse with a world-record net AC efficiency of 53% [19].

To compare with another well-known high-temperature fuel cell, the Molten Carbonate Fuel Cell (MCFC), the all-solid components employed in a SOFC system can avoid issues of corrosion and inability to perform thermal cycling due to the liquid electrolyte used in a MCFC system [23,24]. Therefore, SOFCs have been widely regarded as a technology with operation-friendliness and long service time. In fact, with over 36,750 h (4.5 years) of operation, a Siemens/Westinghouse 100 kWe SOFC–CHP unit has been the longest running fuel cell generator demonstrated to date in the history of fuel cell development [19].

1.1.3. Types of SOFC

Due to the preference for higher performance at lower operating temperatures, recent SOFC designs are typically focused on using a thin electrolyte film supported on conducting porous substrates or channeled dense metal sheets [1–3]. From the materials viewpoint, the substrate can be comprised of electrodes (cathode or anode), interconnect (metal or ceramic) or inactive insulator. From a geometry standpoint, the substrate can be shaped

into either tubular (cylindrical or flattened and ribbed) or planar geometry.

Use of tubular geometry with the one-end closed feature realizes the seal-less design. This is the most marked advantage of tubular geometry over its planar counterpart, where gas seals are necessary to separate air from fuel along the perimeters of cathode–electrolyte–anode and cathode–interconnect–anode [25]. From viewpoint of stacking/bundling, however, one specific type of substrate may be more favorable to combine with one specific type of geometry than another. For example, a cathode substrate with a tubular geometry is an excellent marriage due to its allowance for the cell-to-cell connections in a bundle/stack to occur in reducing atmospheres, where inexpensive transition metals such as Ni can be used [19,25]. Fig. 2 shows a schematic of cell-to-cell connections in a Siemens/Westinghouse cathode-supported tubular SOFC bundle. Otherwise, use of noble metals is necessary to connect single anode-supported tubular cells into a bundle in oxidizing atmospheres. Silver has been the leading choice for this design, but its high mobility and high vapor pressure at high temperatures is problematic to the reliability and stability of anode-supported tubular SOFCs [26–28].

On the other hand, an anode substrate is a good choice for planar SOFC stacks. High-power-density anode-supported single cells enable a reduced operating temperature at which economic and commercially available oxidation-resistant alloys can be utilized to connect single cells into a stack [29,30]. In such a design, the oxidation-resistant alloys have three major functions: mechanical support for the stack, cell-to-cell interconnection and current collection. Fig. 3 shows a schematic of the anode-supported planar SOFC configuration with channeled metal interconnects [9–13]. Gas channels necessary for air and fuel deliveries on a dense metal interconnect are particularly illustrated.

Porous metal substrates representing another class of structural support for SOFCs emerged in recent years [31,32]. The conceivable advantages of metal-supported SOFCs include robustness, easy and low-resistance current collection, and low cost. Technical challenges include how to fabricate a dense electrolyte layer on metal substrates at such a low temperature that excessive oxidation and chemical reactions among the contact layers would not occur.

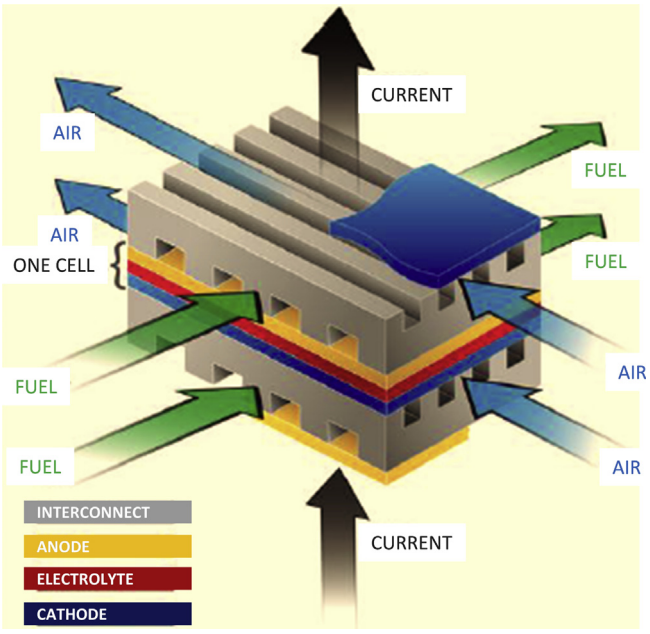

Fig. 3. A schematic illustration of planar SOFC stack with channeled metal interconnect. Courtesy of Fuel Cell Energy, Inc.

Cathode poisoning resulting from high-valence Cr vapor-phase transport and electrochemical condensation at the ORR-active triple-phase boundaries could also potentially degrade the performance [33–36].

Multiple cells can also be connected in series on an electrochemically inactive and electrically insulating porous substrate. This design, termed “segmented-in-series”, has unique advantages such as low fabrication costs (offered by screen printing), and operating the SOFC stacks at high voltage and low current [37,38]. The latter minimizes power losses from current connections, which is of critical importance in large-size SOFC generators. Fig. 4 shows a cross-sectional view of a repeating cell-component unit in

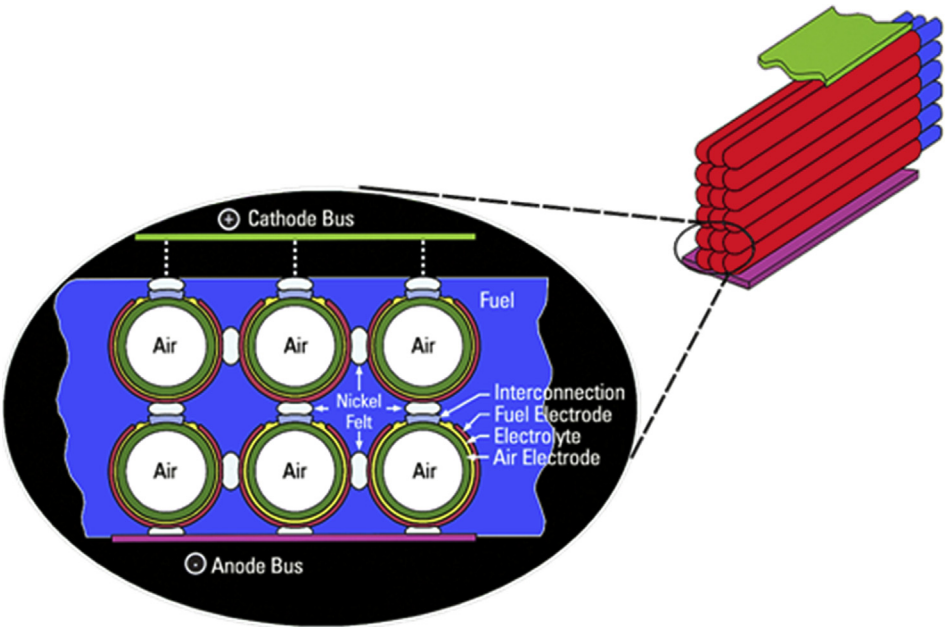

Fig. 2. A schematic illustration of cathode-supported tubular SOFC bundles developed by Siemens/Westinghouse. Courtesy of Siemens Energy, Inc.

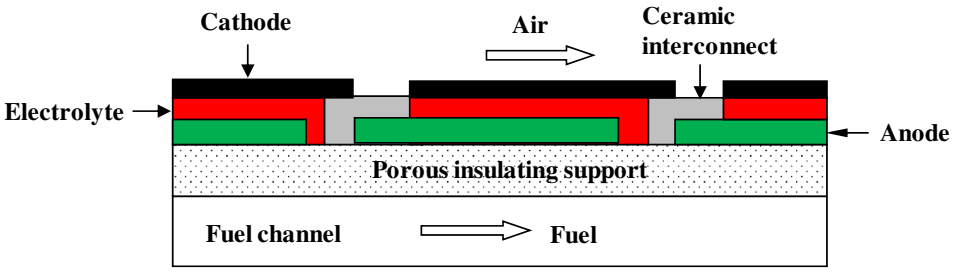

Fig. 4. A schematic illustration of the "segmented-in-series" SOFC design adopted by Rolls-Royce Fuel Cell Systems (now LG Fuel Cells).

"segmented-in-series" design developed by Rolls-Royce [38] and Mitsubishi Heavy Industries (MHI) [39]. Gas manifolding and current collection within the stack are issues remaining to be solved.

1.1.4. Applications

Determined largely by the advantages presented above, the best application of SOFC systems is for the stationary power generation. Depending on the sizes of a SOFC generator, stationary power generation can be further grouped into the following potential markets [1–3]:

- Residential – It is targeted for powering a home with a power rating of 1–10 kW. Hot water, house heating and chilling can also be provided as a by-product. Pipeline natural gas is the fuel of choice. The net AC efficiency is expected to be >35%.
- Industrial – It is targeted for powering a small industrial unit such as a data processing center or a hospital that cannot tolerate a power outage. The power rating typically ranges from 100 to 1000 kW. Quality heat can also be provided as a by-product. Pipeline natural gas or biogas can be used as the fuel. The net AC efficiency is expected to be >45%.
- Dispersed – An extension of industrial SOFC generators can be targeted for powering a larger industrial unit or a small community with a power rating of 2–10 MW. Natural gas, biogas or coal gas is the fuel of choice. The net AC efficiency is expected to be >48%.
- Central – The largest SOFC generator system would have a power rating of at least 100 MW. In such a system, producing electricity by the most efficient way with the lowest carbon emission is the ultimate goal. Therefore, a hybrid SOFC system is the design choice. Natural gas and coal gas can be used as the fuels. The net AC efficiency is expected to be >60%.

1.1.5. Challenges

Despite the promise of SOFCs, product cost and system reliability are the two foremost challenges presently hindering the commercialization of SOFC technology [19,25,40–42]. Both hurdles are essentially rooted in the high operating temperature, a characteristic of SOFCs that has both positive and negative impacts. The high operating temperature allows SOFCs to consume virtually all kinds of hydrocarbon fuels by providing thermal energy for fuel reforming and oxidation. The high operating temperature also generates high-quality heat that can be recovered for primary heat utilization or for secondary electricity production (CHP). On the other hand, high operating temperature requires materials with exceptional properties. Thermal, chemical and electrical incompatibilities among ceramics and metals used in cell components are just a few examples of the pressing issues that need to be addressed in the product development of SOFC technology. Lowering the operating temperature of SOFC from 800–1000 °C to 600–700 °C has been recognized as a practically viable path forward toward commercialization. A great deal of efforts has been devoted to developing intermediate-to-low temperature SOFCs in recent years [43,44].

2. Designs of cathode-supported tubular solid oxide fuel cells

There are five basic components constituting a cathode-supported tubular SOFC: cathode, electrolyte, anode, interconnect and cell-to-cell connector, among which cathode and anode are porous layers allowing transport of gas reactants and products, and electrolyte and interconnect are dense layers separating air and fuel. The major developer of cathode-supported tubular SOFC technology was Westinghouse Electric Corporation, that later became Siemens Energy, in the United States of America, and Toto Ltd. in Japan. The terms "cylindrical" and "flattened and ribbed" are particularly coined in this article to differentiate shapes of the tubes developed by Siemens/Westinghouse [19,25]. The progress made by Westinghouse Electric Corporation in the 1990s has been systematically reported by Singhal in a series of SOFC symposia [45–57].

2.1. Cylindrical tubular single cell design

The earliest prototype of cathode-supported tubular SOFCs was demonstrated by Westinghouse from 1962 to 1963 in a stack design called "bell-and-spigot" [58]. The poor stability and complex manufacturing of this design led to the birth of cylindrical Porous Support Tube (PST) made of Ca-doped ZrO_2 to support layers of cathode, electrolyte, anode and interconnect [19,59]. The PST was later replaced by a porous cathode substrate to support other functional layers, which since became the foundation of later cathode-supported tubular SOFC technology [19]. This design change markedly improved cell performance by reducing the gas-diffusion resistance and sheet resistance arising from the cathode substrate [19]. Fig. 5 illustrates the basic configuration of a Siemens/Westinghouse cathode-supported, one-end-closed tubular SOFC design.

2.2. Flattened ribbed tubular single cell design

One of the shortcomings associated with the cylindrical tubular geometry is the long current pathway along the circumference of the circular cross section, resulting in higher ohmic resistance. To circumvent this problem, an alternative design was proposed in the mid-1990s by Westinghouse Electric Corporation [55]. The important feature of this new design was the shortened current pathway by flattening the circular cross-section into a rectangular shape in conjunction with multiple ribs connecting the two flattened surfaces; the formed cavities were still used as the channels for air delivery. This type of cells was known as High Power Density or HPD cells. In the literature, the cell designation was often seen attached with a figure denoting the number of air channels. Fig. 6 shows an exemplary schematic of HPD5 design, which possesses five air channels [55].

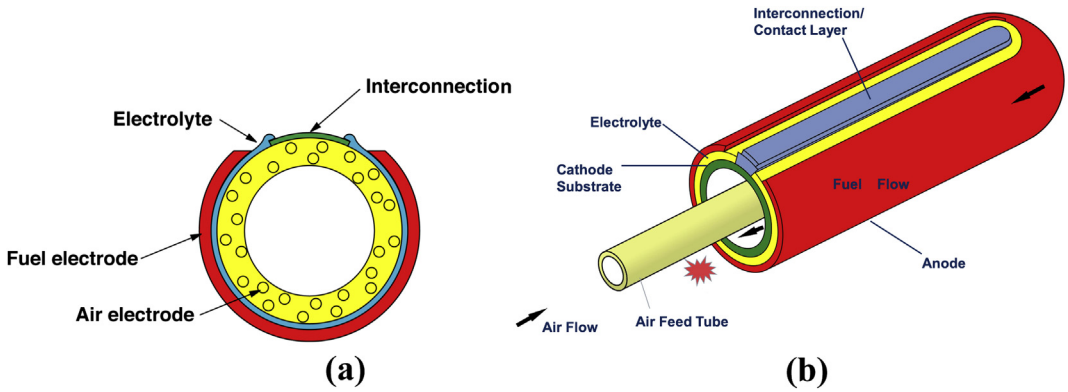

Fig. 5. A schematic of single cathode-supported tubular SOFC. (a) Cross-sectional view; (b) three-dimensional view of the cell. Courtesy of Siemens/Westinghouse.

It is conceivable that a variety of geometrical parameters of the HPD cathode substrates, such as cell width, wall thickness, rib height, and number of ribs, can be varied to optimize the performance. When performing the engineering design, both the electrical performance and mechanical strength need to be considered [60]. For example, a wider and thinner HPD cell can produce more power at higher power density due to a shorter current path length and larger surface area. However, such a HPD design may not possess sufficient mechanical strength, thus compromising durability. In addition, smaller air channels could elevate the pumping power for air delivery, thus reducing the net efficiency of system. Therefore, optimization of HPD cell geometry is a multi-scale design process involving all perspectives of electrochemistry and mechanics.

Over the years, engineers at Westinghouse and Siemens systematically investigated the effect of geometrical parameters of HPD cells on the electrical performance and thermal stress distribution [60]. These fundamental works led to the creation, pilot-scale production and comprehensive electrical and mechanical testing of HPD5 and HPD10 cells in the late 1990s to early 2000s. The HPD5 design featured larger air channels and longer current path length than the HPD10, resulting in lower power density but stronger HPD5 than HPD10.

Another noteworthy advance in Siemens/Westinghouse during the 2000s was the development of Delta Cells, an alternative version of HPD cell featuring increased surface area for high power output without compromising the specific power density by making the active surface in wavy shape [60–63]. The triangular geometry of these Delta Cells automatically provided flow fields for both air and fuel. The adoption of Delta8 (eight air channels) design represented a significant increase in cell surface area. Table 1 compares the primary geometrical parameters of Siemens/Westinghouse's cathode-supported tubular SOFCs [19,25,60]. However, the increase in surface area and therefore in total power output comes at the expense of lowered mechanical strength. The stress concentration points are usually located at the valley joints between two adjacent triangles. Therefore, the Delta cells are generally considered less robust than HPD cells.

The progression of Siemens/Westinghouse's HPD cell geometries driven by the demands for high power density and power output is illustrated in Fig. 7.

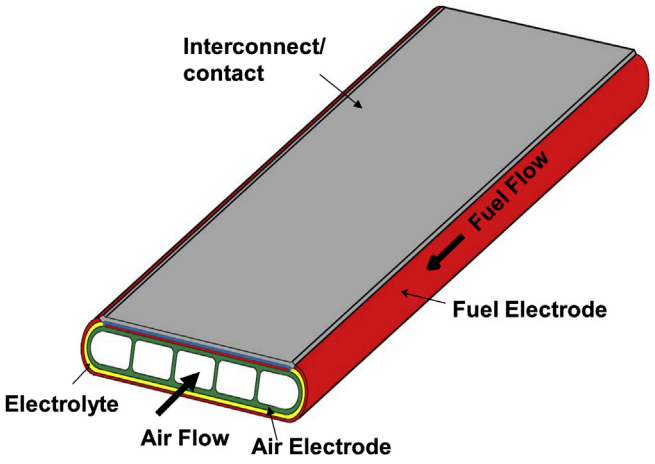

Fig. 6. A schematic illustration of HPD5 design developed by Siemens/Westinghouse. Courtesy of Siemens/Westinghouse.

2.3. Cylindrical tubular bundle design

As aforementioned, a single SOFC produces a low voltage of little practical use. To make SOFCs into a useful power generation device, each individual cell needs to be connected in series to raise the voltage and in parallel to boost the current. For cathode-supported tubular SOFC systems developed by Siemens/Westinghouse, a bundle consisting of 3 cells in parallel and 8 cells in series (often termed "3 × 8 bundle") was designed as the building block for scaled up systems [61–63]. For example, a 200 kW CHP–SOFC generator contains 1152 cells in an array of forty-eight 3 × 8 bundles [19,25]. A typical 3 × 8 bundle is illustrated in Fig. 2.

2.4. Flattened ribbed tubular bundle design

For flattened ribbed tubular bundles, parallel connection was impossible due to the geometrical limitation. Therefore, the bundle design was simple, all in series. Such a bundle design also made sense since there was no need to boost current by parallel connection for single cells capable of producing high current. The number of single cells in a bundle was then determined by the rating and footprint of the generator, mechanical strength of cell and ease of assembly. Fig. 8 shows an example of 1 × 8 (8 cells connected in series) bundle made from Delta8 cells, capable of producing 5 kW power [61–63].

Table 1
Major geometrical parameters of Siemens/Westinghouse SOFCs.

	Cylindrical	HPD5	HPD10	Delta9	Delta8
Length (cm)	150	75	75	75	75
Width (cm)	Inner $D = 1.8$ Outer $D = 2.2$	10	10	10	15
Effective surface area (cm^2)	834	830	810	1250	2100

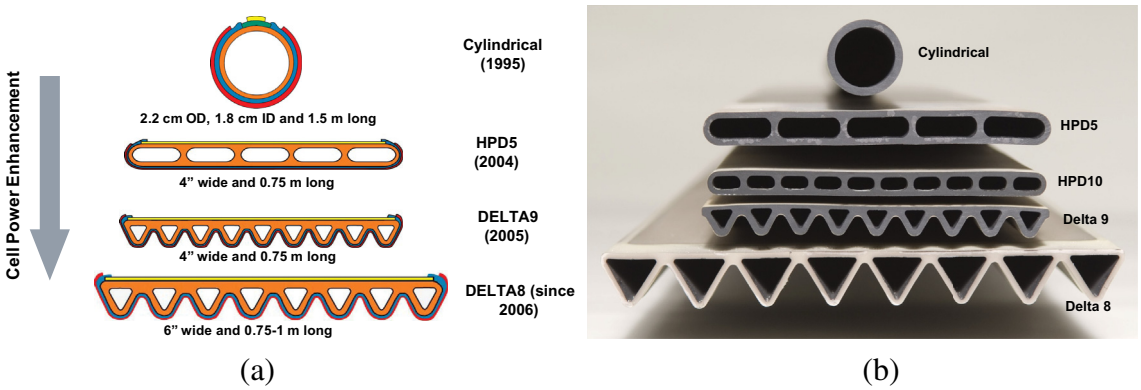

Fig. 7. Schematic (a) and actual image (b) of HPD and Delta cells developed in Siemens/Westinghouse from the 1990s to 2000s. Courtesy of Siemens/Westinghouse.

3. Cell materials and manufacturing process of cathode-supported tubular SOFCs

Materials for cell components and fabrication techniques for manufacturing a complete functional cathode-supported tubular SOFC are reviewed in this section.

3.1. Cell materials

The Siemens/Westinghouse cathode-supported SOFCs employed materials developed at Westinghouse from 1960s to mid-1980s, and widely known to the SOFC community as the state-of-the-art materials. Table 2 lists these materials for each functional component, along with their thickness [19]. The selection of cell materials was primarily based on two critical criteria: electrical conductivity and thermal expansion coefficient [19,25]. The latter was the primary reason for Siemens/Westinghouse to select Ca instead of Sr as the dopant for $LaMnO_3$ and $LaCrO_3$; Ca-doping can produce a better matched thermal expansion coefficient to that of ZrO_2-based electrolytes. This consideration was a tradeoff between mechanical compatibility and electrical performance since Sr-doped perovskites usually give higher electrical conductivity and electrocatalytic activity but higher thermal expansion coefficients than Ca-doped counterparts.

3.2. Cell manufacturing process

The manufacturing process for each functional layer in a SOFC largely depends on the SOFC design. The criteria for adopting a specific manufacturing technique over others need to consider cost effectiveness, viability for mass production and automation, processing repeatability, and precision. In this section, fabrication techniques particularly used for making Siemens/Westinghouse's cathode-supported tubular SOFCs are reviewed.

3.2.1. Substrate

A substrate in a SOFC is a mechanical support that provides a vehicle on which functional thin layers can be sequentially deposited. Therefore, it must be mechanically strong, chemically stable, and thermally matched to other layers. The cathode substrate developed by Siemens/Westinghouse in the form of a cylindrical tube to support films of electrolyte, anode, and interconnect was fabricated by extruding a ceramic paste through a mold to a desirable diameter (inner and outer) and length [25]. The paste was a mixture of proprietary cathode powders, solvent, organic binder, and pore former. After appropriate drying, the tube went through a two-step sintering process: lower temperature horizontal bisque firing and higher temperature hang firing, to yield a ceramic body with a well-defined microstructure containing sufficient porosity and distribution, and, most importantly, good mechanical strength. Fig. 9 shows a representative microstructure of such a substrate, where a roughly 30–35% of porosity is present. To ensure the quality of the substrate, chemical composition, dimensionality, mechanical strength, thermal expansion coefficient, thermal cycling shrinkage and porosity were closely monitored during each batch production.

3.2.2. Electrolyte thin film

Fabrication of quality electrolyte thin films is the most important step of all stages involved in the production of a SOFC. The requirement for a thin and dense coating challenges the

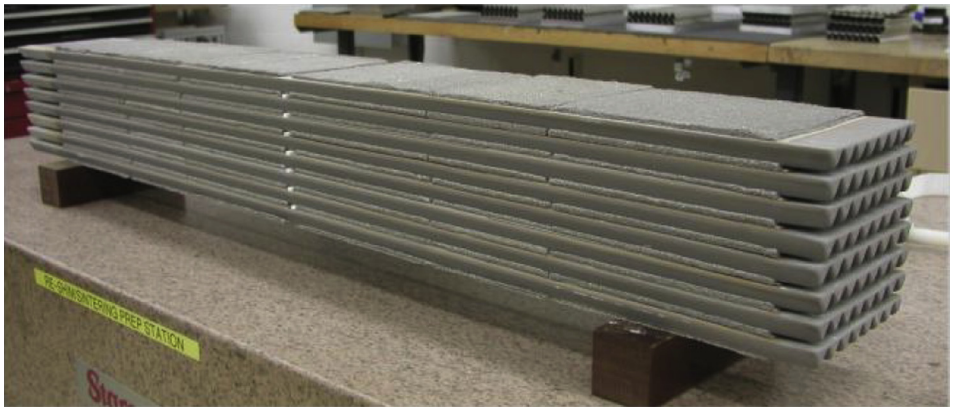

Fig. 8. A 1 × 8 Delta8 bundle capable of producing 5 kW power. Courtesy of Siemens/Westinghouse.

Table 2
Cell materials employed in Siemens/Westinghouse cathode-supported tubular SOFCs.

Component	Material	Thickness
Cathode	Ca- and Ce-doped $LaMnO_3$	2.2 mm wall thickness
Electrolyte	Y_2O_3- or Sc_2O_3-doped ZrO_2	40–60 μm
Anode	Ni-electrolyte cermet	100 μm
Interconnect	Ca- and Al-doped $LaCrO_3$	100 μm

conventional ceramic fabrication techniques. These techniques can be generally classified into three categories: vapor deposition (e.g., EVD and PVD), thermal spray (e. g., atmospheric plasma spray) and slurry coating (e. g., colloidal deposition, slip casting, screen printing, electrophoresis deposition, wet powder spray, and so on).

The electrolyte thin-film fabrication technique adopted by Siemens/Westinghouse experienced a gradual transition from the early EVD (Electrochemical Vapor Deposition) process invented in 1977 to today's APS (Atmospheric Plasma Spray) process developed since 2000s [19,25,64–66]. This change was primarily driven by the cost and productivity considerations for large-scale mass production. The main steps of the EVD process are schematically illustrated in Fig. 10 [66].

As the gaseous mixture of $ZrCl_4$ and YCl_3 is fed to the outer surface of the tubular cathode substrate and steam is introduced to the inner surface at elevated temperatures, the chemical reaction first occurs at the locations where they meet, namely pores, by [64–66]

$$\begin{aligned} ZrCl_4 + 2H_2O &\rightarrow ZrO_2 + 4HCl \\ 2YCl_3 + 3H_2O &\rightarrow Y_2O_3 + 6HCl \end{aligned} \quad (1)$$

Since the gas diffusion process in the substrate is the rate-limiting step, the growth of the initial layer that closes the surface pore is linear with time. As soon as the surface pores are closed, the oxide-ion and electronic conduction in the initially formed 8YSZ at elevated temperature under a gradient of oxygen chemical potential comes into play: an oxygen flux that counterbalances the electronic flux is generated. This process can be best described by the following electrochemical reactions

$$\begin{aligned} ZrCl_4 + 2O_O^{\times} &\rightarrow ZrO_2 + 2Cl_2 + 2V_O^{\cdot\cdot} + 4e' \\ 2YCl_3 + 3O_O^{\times} &\rightarrow Y_2O_3 + 3Cl_2 + 3V_O^{\cdot\cdot} + 6e' \end{aligned} \quad (2)$$

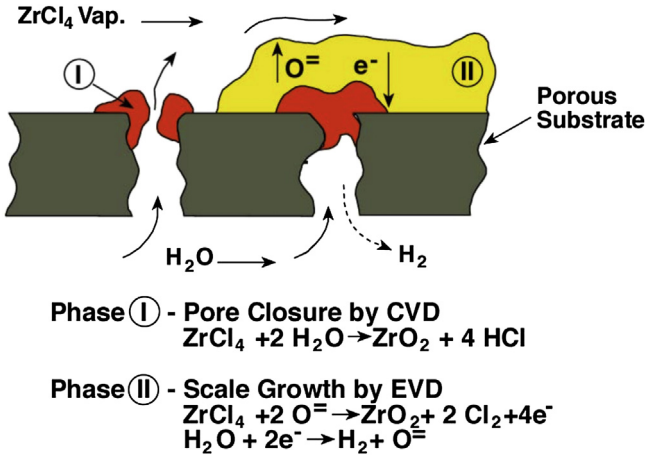

Fig. 10. Illustration of the principle of the EVD process. Courtesy of Siemens/Westinghouse.

where $O_O^{\times}$, $V_O^{\cdot\cdot}$ and e' represent regular oxygen lattice (O^{2-}), oxygen vacancies and free electrons, respectively. As a result, a film of 8YSZ continues to grow; the growth rate k_p is governed by the classical parabolic rate law (Wagner equation). The relationship between thickness L and time t can, therefore, be given by

$$L^2 = 2k_p t \quad (3)$$

At a typical EVD temperature of 1000–1200 °C, the rate constant for deposition of 8YSZ ranges from 1.1×10^{-5} to 3.8×10^{-3} $cm^2\ s^{-1}$ [66]. Considering both initial linear and later parabolic growth rate, to achieve a 40 μm 8YSZ-film takes approximately 40 min at 1000 °C and 20 min at 1200 °C. Fig. 11 shows a representative microstructure of an EVD electrolyte. It is evident that the EVD process is capable of producing pinhole-free, thin and dense electrolyte films in the range of micrometers.

The major drawback of the EVD process was the high cost associated with labor, materials, waste disposal and maintenance incurred during mass production. After successful demonstrations of several SOFC generators based on EVD electrolytes and anodes by Westinghouse in the 1990s [19], this cost-prohibitive technique was later replaced by the more productive and automation-friendly APS coating technique.

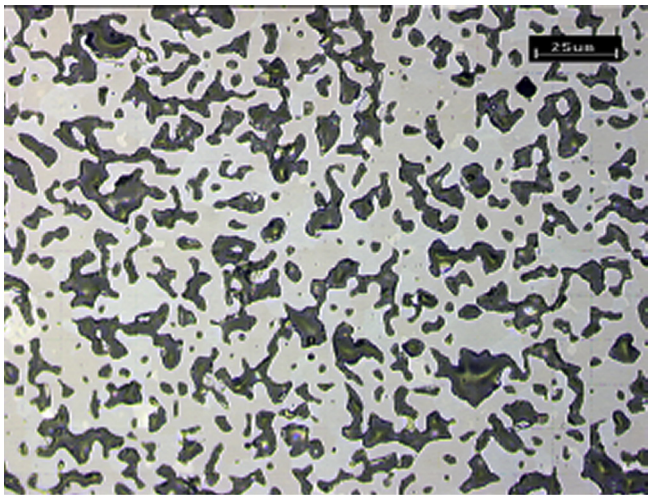

Fig. 9. Typical microstructure of a Siemens/Westinghouse cathode substrate after sintering. Courtesy of Siemens/Westinghouse.

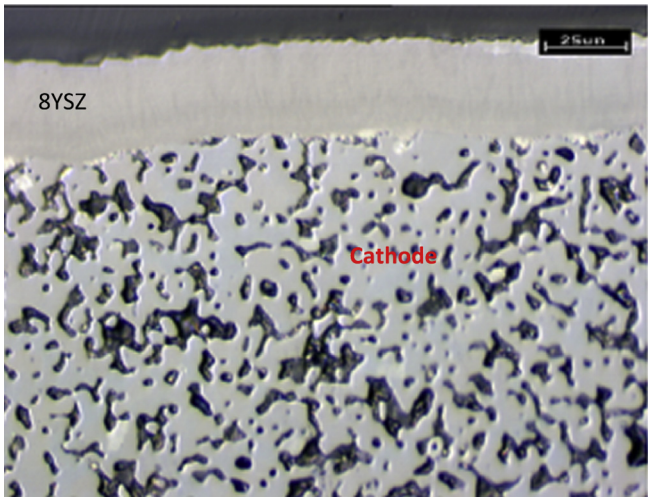

Fig. 11. Microstructure of an EVD electrolyte on the porous cathode substrate. Courtesy of Siemens/Westinghouse.

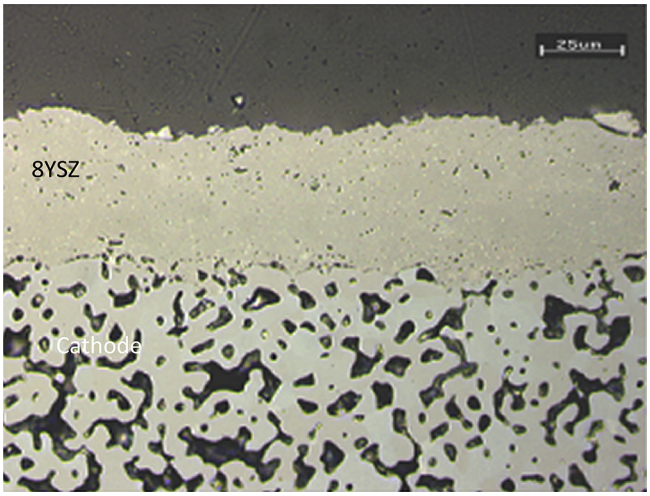

Fig. 12. Typical microstructure of an APS electrolyte on a porous cathode substrate. Courtesy of Siemens/Westinghouse.

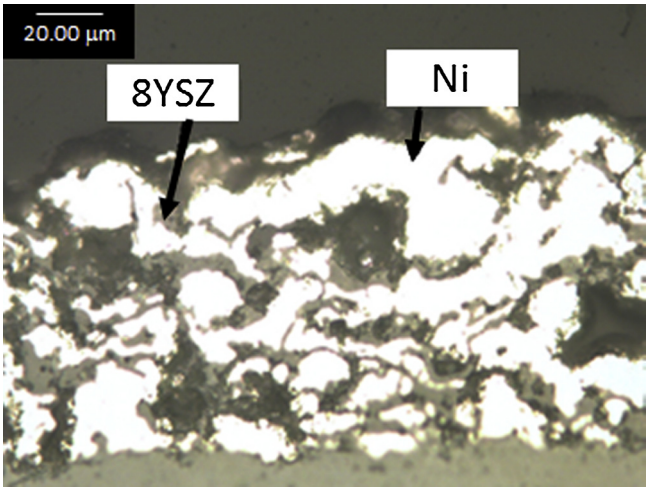

Fig. 14. Microstructure of an anode made by the APS process. Courtesy of Siemens/Westinghouse.

Application of the APS technique to fabricate electrolyte films on a porous cathode substrate was first experimented in Westinghouse in the late 1990s [25]. Plasma spray is a well-established technology to manufacture a variety of coatings on different substrates. The primary advantage of this technology is its ability to produce well-bonded and high-density coatings [67]. The process involves formation of a very high temperature plume by ionized gas and simultaneous injection of particles to be deposited. The resultant molten or heat-softened particles are subsequently propelled at a high velocity toward the substrate and rapidly solidified on the substrate's surface. After extensive parametric studies on gun power, primary and secondary gas flows, powder feed rate and cooling effect, Siemens/Westinghouse eventually qualified the processing conditions in the mid 2000s for fabricating 8YSZ layer with APS. Fig. 12 shows a representative microstructure of plasma-sprayed 8YSZ on a porous cathode substrate. The shown microstructure was gastight with a small fraction of closed pores.

It was generally found that the mechanical strength of the APD cells is less dependent on these closed pores than the cathode substrates. The APS electrolyte films deposited are typically under an intense compressive stress created by the rapid solidification of melted electrolyte power [68]. On the other hand, the magnitude of ionic conductivity of APS electrolytes shows no significant difference from that of EVD ones in 900–1000 °C. However, EVD electrolytes exhibit lower activation energy for ionic conduction than the APS electrolytes, resulting in its higher ionic conductivity at lower temperatures. Higher post-spray sintering temperature for APS electrolytes is deemed the root-cause for the behavior.

3.2.3. Anode thin film

The anode layer was also produced by EVD process (called "fuel fix") in the early SOFC systems based on EVD electrolytes [19,25]. Fig. 13 shows a representative microstructure of EVD anode. The EVD-made 8YSZ elegantly coated on the surface of a porous Ni-network, fulfilling the requirements for maximizing triple-phase boundaries and limiting the coarsening of Ni-particles. During the transition to APS coating technique, Westinghouse/Siemens also demonstrated that the anode layer in a cathode-supported tubular SOFC can also be fabricated by the APS. A powder mixture of metallic Ni, pore former and YSZ was used as the feedstock. One of the advantages of the APS anode was that no additional sintering

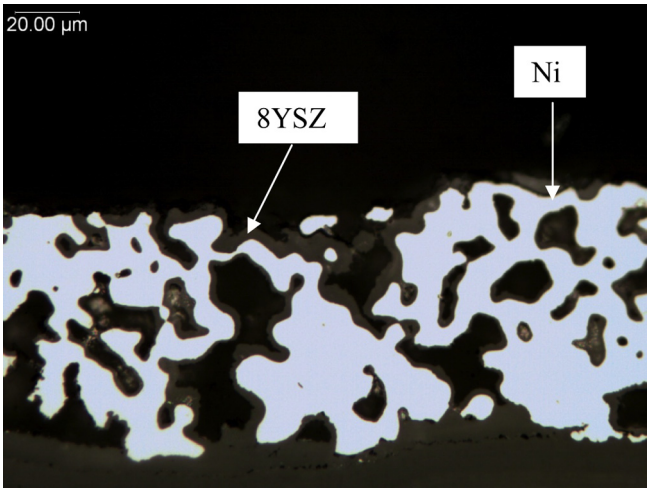

Fig. 13. Ideal porous microstructure exemplified by an EVD-made anode. Courtesy of Siemens/Westinghouse.

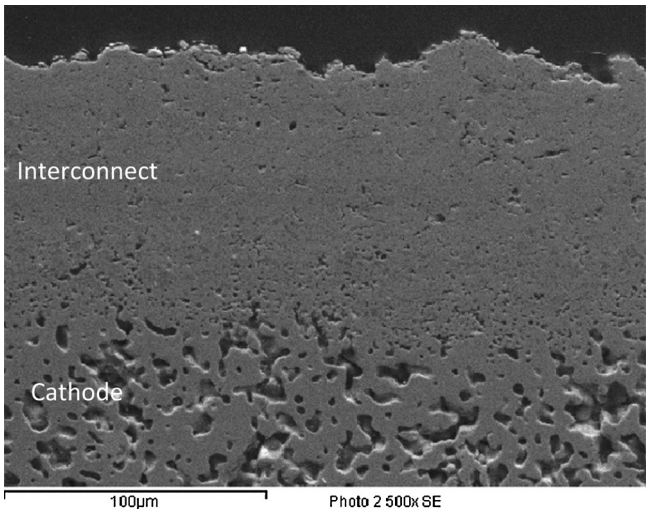

Fig. 15. Microstructure of $LaCrO_3$-based interconnects fabricated by the APS process. Courtesy of Siemens/Westinghouse.

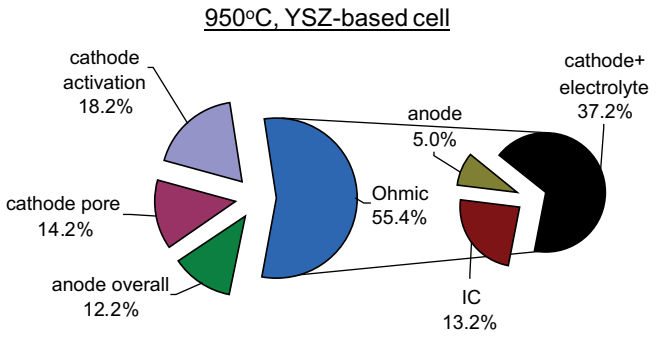

Fig. 16. Cell ASR distribution of a cathode-supported tubular SOFC developed by Siemens/Westinghouse. Courtesy of Siemens/Westinghouse.

step was necessary after APS processing. A representative microstructure of the APS anode is illustrated in Fig. 14. The slurry dip-coating method was used by Toto as a low-cost process to make the anode, followed by drying and co-sintering steps [69].

3.2.4. Interconnect thin film

The ceramic $LaCrO_3$-based interconnects are generally difficult to sinter due to the "vaporization-condensation" mechanism of Cr–O species during the sintering process, which causes coarsening of the particles preventing densification [70]. To alleviate the Cr-volatilization problem, A-site excess or Cr-deficiency in $LaCrO_3$ were generally formulated to promote sintering by forming multi-phase chromates that melt incongruently in the range of 1000–1200 °C [71]. This strategy was eventually engineered by Westinghouse into the interconnect APS process [72]. Fig. 15 shows a representative microstructure of an APS interconnect layer on a porous cathode substrate. Again, the layer deposited was gastight with a small fraction of closed pores.

4. Electrical performance of cathode-supported tubular solid oxide fuel cells

It is well known that cathode-supported tubular SOFCs generally have inferior performance compared to anode-supported planar counterparts due to higher ohmic as well as cathode polarization resistances. Cell power enhancement, therefore, remained a paramount priority for Siemens/Westinghouse product development for many years [19,25]. The significance of cell power enhancement is unequivocal: cost ($ kW^{-1}) reduction, which has driven many Siemens/Westinghouse internal as well as DOE-funded programs toward this direction [19,25]. Based on the distribution of cell resistance among cell components shown in Fig. 16, where cathode-related ohmic and polarization area-specific resistances (ASRs) account for ~32% and ~37% of the total cell ASR at 950 °C [73], two major programs were implemented by Siemens/Westinghouse in the course of product development: 1) application of advanced cell materials including composite interlayer at the cathode/electrolyte interface and high conductivity ScSZ electrolyte as an effort to reduce cell total ASR, and 2) development of HPD/Delta cells to reduce cell total ASR as well as increase the effective surface area for increasing power output per unit cell [73]. The potential reduction in cell ASRs according to Fig. 16 could be as much as 72%, the accomplishment of which can significantly enhance the cell power output.

To ensure the comparativeness of each electrical test, Siemens/Westinghouse also established a standard test protocol over years' development. The standard testing conditions were recorded as: fuel inlet composition 11%H_2O–H_2, fuel utilization (U_f) 80–85%, air utilization (U_o) 16–20%, and lowest cutoff cell voltage 0.5 V [74–76].

4.1. Single cell tests

Over one thousand electrical tests were performed in Siemens/Westinghouse over several decades of product development. The cells tested ranged from the early PST cells with EVD electrolytes and anodes to today's cathode-supported APS electrolytes and anodes, in both cylindrical and HPD/Delta tubular geometries. These cells had a linear length ranging from 50 to 1000 cm of either cylindrical or HPD/Delta tubular shape, and were characterized over a broad spectrum of temperature, current density, fuel utilization, and air utilization. Fig. 17 summarizes *V–I* characteristic of cylindrical and HPD/Delta tubular cells developed in recent years by Siemens/Westinghouse, tested under conditions of 900–950 °C, U_f = 80% and U_o = 20% [73]. This composite plot unambiguously shows a marked progressive improvement in cell power

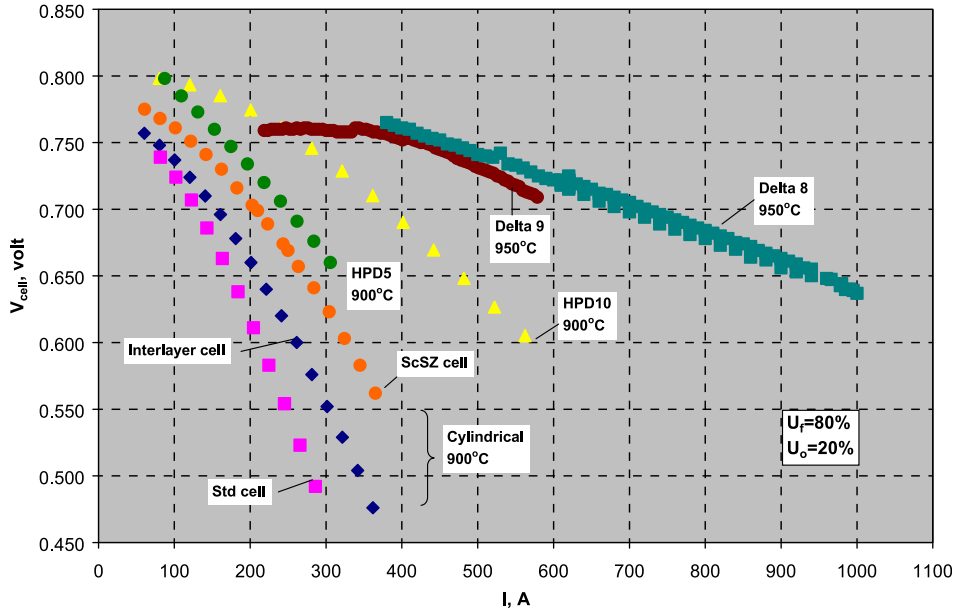

Fig. 17. Comparison of *V–I* characteristic of standard and advanced cylindrical and HPD tubular SOFCs. Courtesy of Siemens/Westinghouse.

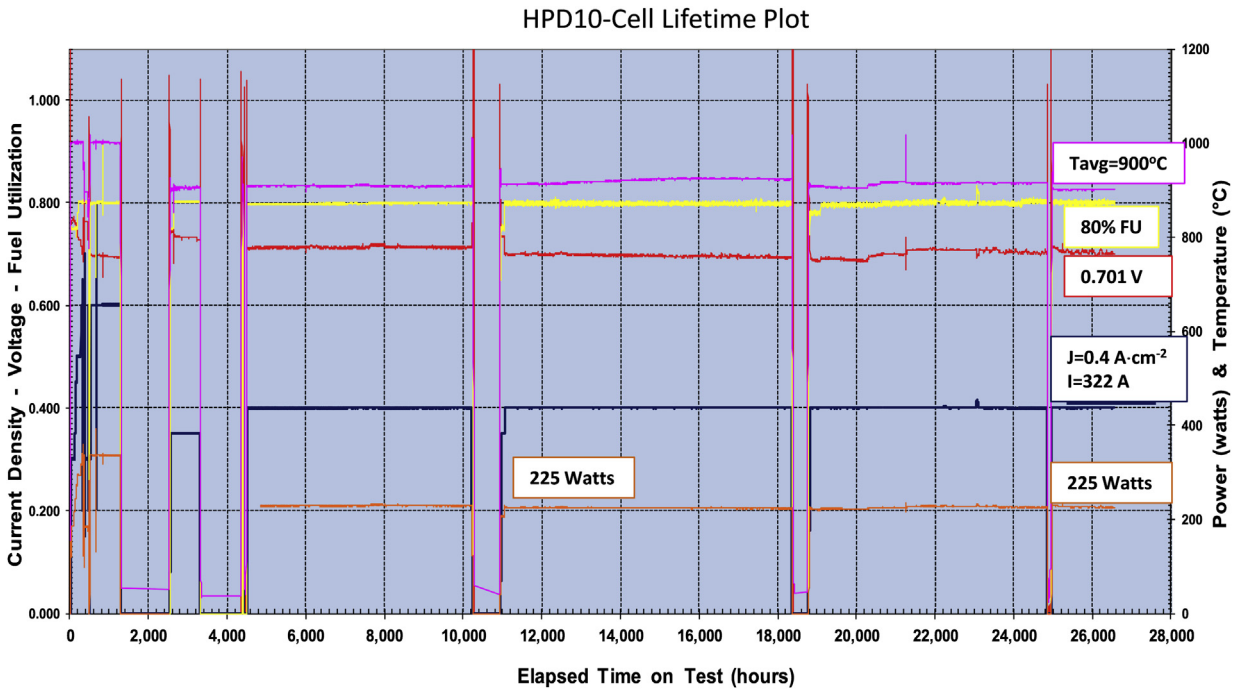

Fig. 18. Long term plot of a HPD10 cell operated at 900 °C. Courtesy of Siemens/Westinghouse.

by implementing advanced materials (cathode interlayer and Sc-doped ZrO_2 or ScSZ electrolyte) and transitioning to HPD/Delta geometries.

Another highlight of Siemens/Westinghouse's cathode-supported SOFCs was their excellent long-term stability. Fig. 18 shows a long-term test on a 75-cm long HPD10 cell consisting of a ScSZ electrolyte and ScSZ/cathode composite interlayer. Over 26,000 h (~3 years) under 900 °C, $U_f = 80\%$ and 322 A, the cell only showed a degradation rate of 0.02% per 1000-hour, a performance unmatchable by any other designs of SOFCs in the history of SOFC development [61,62].

4.2. Bundle tests

Only the electrical performance of HPD/Delta bundles is reviewed here. The performance of a standard 3 × 8 cylindrical

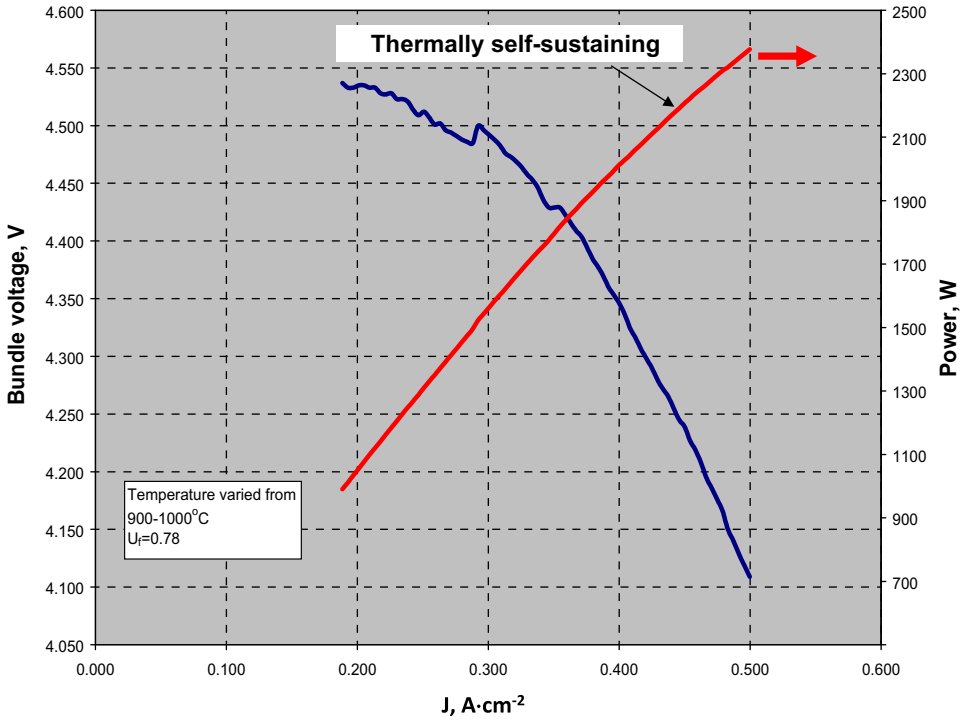

Fig. 19. *V–J* characteristic of a 1 × 6 Delta9 bundle. Courtesy of Siemens/Westinghouse.

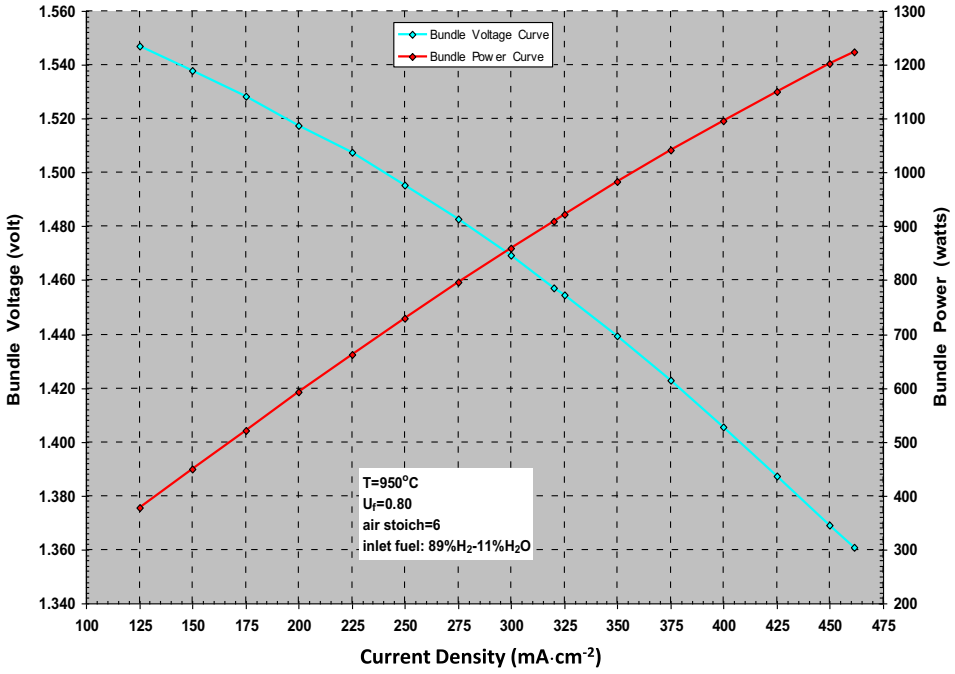

Fig. 20. The *V–J* characteristic of a 1 × 2 Delta8 bundle. Courtesy of Siemens/Westinghouse.

tubular bundle producing ~2.4 kWe is used as the baseline to compare with the performance of HPD/Delta bundles in the following context.

Fig. 19 shows *V–J* characteristic of a 1 × 6 (six cells in series) Delta9 bundle tested under the nominal condition [73]. Within the testing enclosure consisting of muffle tube and heating elements, a combination of air flow at $U_o = 20\%$ and heat from H_2-oxidation and joule heating yielded a temperature distribution of 900–1000 °C along the length of the cell. At $J = 0.5$ A cm^{-2}, the highest current density operated without reaching the peak power, the power output achieved ~2.4 kWe. This is an equivalent performance to a standard 3 × 8 cylindrical bundle but accomplished by only six Delta9 cells. Also interesting to note was the bundle performing in thermally self-sustaining manner at $J = 0.45$ A cm^{-2} or ~2.2 kWe power. At this point, all heating elements of the furnace had zero output.

Further power enhancement by Delta8 cells is shown in Fig. 20, where the *V–I* characteristic of a 1 × 2 bundle Delta8 bundle tested under the standard conditions indicates a power output of 1.2 kWe at $J = 0.45$ A cm^{-2}. An extrapolation of this performance suggests that only four Delta8 cells were needed in a 1 × 4 bundle to produce an equivalent 2.4 kWe of one standard cylindrical 3 × 8 bundle.

5. System demonstrations

A complete Siemens/Westinghouse SOFC system typically consisted of three major subsystems: stack, module and BOP (Balance-of-Plant). The stack has been discussed above. The module includes insulation materials, fuel reformer, fuel nuzzle, combustion plenum, fuel plenum and other components surrounding the stack. Fig. 21 shows a schematic of Siemens/Westinghouse SOFC module. The BOP system typically includes the process control, power conditioning, desulfurizer and gas supplies.

5.1. SOFC generators based on EVD cells

Over the past half-century, Westinghouse, later Siemens, developed and demonstrated a total of 28 SOFC generators ranging from 0.4 to 200 kW in USA, Japan and Europe [18–20,77–81]. The majority of those successfully demonstrated units were before 2003, when only EVD cells were employed in the generators.

The cornerstone demonstration of high-efficiency SOFC generator systems was the atmospheric 100-kWe class SOFC–CHP system, shown in Fig. 22. It was the first field unit to utilize the commercial cathode supported cells (22 mm diameter, 150 cm active length, 834 cm^2 active area) and in-stack reformers. It consisted of a 24-cell array arranged as eight cells in electrical series by three cells in electrical parallel as shown in Fig. 2. It was operated on natural gas by EDB-ELSAM (a Dutch/Danish utility consortium), producing between 105 and 110 kWe net AC to the utility grid and approximately 65 kW to the hot water district heating system. In addition, the system achieved an impressive 46% electrical

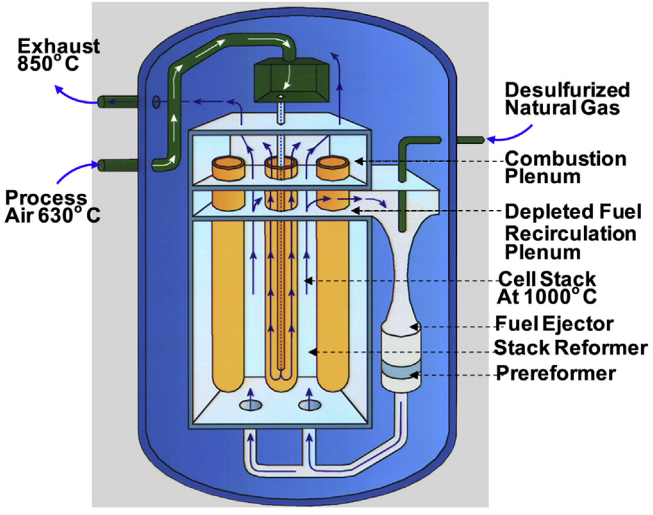

Fig. 21. A schematic of Siemens/Westinghouse SOFC module configuration. Courtesy of Siemens/Westinghouse.

Fig. 22. The 100-kWe class SOFC generator system. Courtesy of Siemens/Westinghouse.

efficiency (net AC/LHV) in the Spring/Summer of 1999, and accumulated ~13,000 testing hours [19]. The same unit after partial repairs was operated in Italy and Germany for additional tens of thousands hours. Table 3 lists the demonstrated SOFC generators produced by Westinghouse before 2003.

Another cornerstone demonstration of the very high efficiency SOFC generator was the pressurized SOFC/gas-turbine hybrid (PSOFC/GT) system sponsored by Southern California Electricity (SCE) and U. S. Department of Energy. The stack design of PSOFC/GT was the same as EDB/ELSAM operated at 3 atm absolute pressure for 3257 h, producing 190 kWe electricity from the SOFC stack and 30 kWe from the gas-turbine with 53% AC net efficiency, the highest ever among all types of power generation systems [19]. Fig. 23 shows the PSOFC/GT system.

Another noteworthy development during the late 1990s and early 2000s was the conceptual design of a "zero-emission" SOFC power systems employing CO_2 sequestration. The anode exhaust stream containing only steam and CO_2 allows an easy capture and sequestration of CO_2, making the efficient and pollution-free SOFC-based power plants possible [82].

5.2. SOFC generators based on APS cells

Since 1998 when Siemens acquired Westinghouse's tubular SOFC technology, the product development shifted toward developing fabrication techniques that were more mass-production friendly and viable than the EVD process. The costly and production-unfriendly EVD process was gradually displaced by the APS process after an extensive and lengthy qualification process [25]. The viability of APS technique for making SOFC components was first demonstrated on cylindrical tubular cells in smaller systems CHP5 that contained four 2 × 11 bundles (87 cm long cell), producing nominal 5 kWe with heat recovery. The longest running generator based on APS cells was demonstrated in Johnstown, Pennsylvania for over 10,000 h with natural gas as the fuel. Following this success, a dozen or more CHP5 SOFC generators were ordered by customers worldwide, one of which was successfully demonstrated in Phipps Conservatory of Pittsburgh for over 5000 h using natural gas as the fuel and feeding the produced CO_2 and H_2O to a botanical garden. Fig. 24 shows an external look of the smaller CHP5 SOFC system.

Table 3
Summary of demonstrated Westinghouse's SOFC generator systems before 2003.

Year	Country	Customer	Rating (kWe)	No. of stack	Cell type	Cell length (mm)	No. of cells	Operation hours	Fuel	MWh (DC)
1986	USA	Tennessee Valley Authority	0.4	1	PST	300	24	1760	$H_2 + CO$	0.5
1987	Japan	Osaka gas	3	1	PST	360	144	3012	$H_2 + CO$	6
1987	Japan	Osaka gas	3	1	PST	360	144	3683	$H_2 + CO$	7
1987	Japan	Tokyo gas	3	1	PST	360	144	4882	$H_2 + CO$	10
1992	Japan	JGU-1	20	2	PST	500	576	817	PNG	11
1992	Japan	Utilities-A	20	1	PST	500	576	2601	PNG	36
1992	Japan	Utilities-B1	20	1	PST	500	576	1579	PNG	26
1993	Japan	Utilities-B2	20	1	PST	500	576	7064	PNG	108
1994	USA	SCE-1	20	1	PST	500	576	6015	PNG	99
1995	USA	SCE-2	27	1	AES	500	576	5582	PNG/DF-2/JP-8	118
1995	Japan	JGU-2	25	1	AES	500	576	13,194	PNG	282
1998	USA	SCE-2/NFCRC	27	1	AES	500	576	3394+	PNG	73+
1997	Netherlands	EDB/ELSAM-1	125	1	AES	1500	1152	4035	PNG	471
2000	Netherlands	EDB/ELSAM-2	125	1	AES	1500	1152	12,576	PNG	1477
2002	Germany	RWE	125	1	AES	1500	1152	3870	PNG	498
2003	USA	SCE(PH220)	200	1	AES	1500	1152	3257	PNG	472

PST: porous support tube (Ca-doped ZrO_2); AES: air-electrode support; PNG: pipe natural gas.

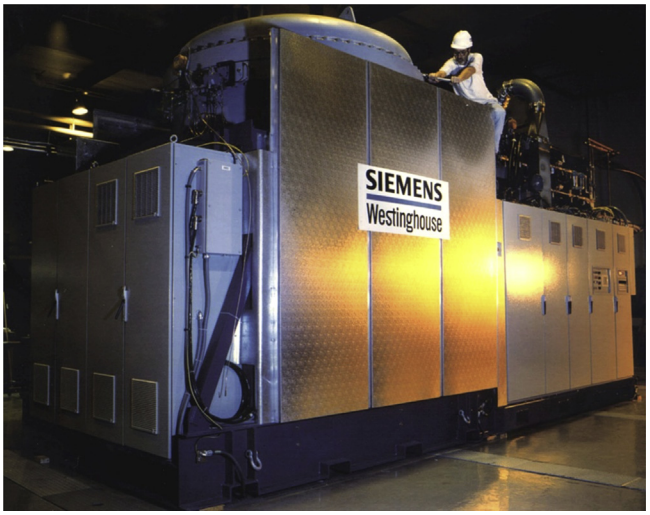

Fig. 23. The 200-kWe class pressurized hybrid SOFC/micro-turbine generator. Courtesy of Siemens/Westinghouse.

Despite the success of CHP5 systems, the development of scaled up systems based on APS cells was not very successful; simultaneous changes from EVD to APS and cylindrical to HPD/Delta cells caused a lot of uncertainties in product quality, yields and reliability. This was reflected in a DOE-SECA funded program to develop HPD SOFC generators for a 25 kWe system [61]. The stack shown in Fig. 25 containing 32 Delta8 cells in four 1 × 8 array failed at an electrical loading of ~15 kW due to local cracks in the cathode substrate originating from stresses developed from current loading (lattice oxygen reduction caused lattice expansion).

Fig. 24. A CHP5 SOFC generator. Courtesy of Siemens/Westinghouse.

Fig. 25. Four 1 × 8 Delta8 bundle stack for 25 kWe unit. Courtesy of Siemens/Westinghouse.

6. Concluding remarks

More than 150 years has passed since the original concept of fuel cell was first proposed. It gives a mixed feeling when observing that this simple-in-principle and efficient-in-energy conversion device still requires considerable engineering development in order to become a commercially viable product. High product cost that is unable to compete with conventional ICEs is the major challenge to the commercialization of SOFCs. Application of advanced materials and cost-effective fabrication techniques represents an effective means of cost reduction and power enhancement. A viable approach should be lowering the operating temperature from current 900–1000 °C to 600–800 °C range, where low-cost cell as well as module materials can be employed, along with improved cell reliability. As a multi-component system, the expenditures of BOP and module also contribute to a significant portion of the final product cost. Therefore, cost reduction in these areas would also be necessary.

Nevertheless, over a half-century of development, Siemens/Westinghouse demonstrated the world first longest running, highly efficient 100 kWe class SOFC–CHP system and the first 200 kWe class PSOFC/GT power generation system with its unique cathode-supported tubular SOFC technology. These engineering achievements will never be forgotten in the history of SOFC development.

References

[1] K. Huang, J.B. Goodenough, Solid Oxide Fuel Cell Technology: Principles, Performance and Operations, Woodhead Publishing Ltd., Cambridge, UK, September 2009.
[2] N.Q. Minh, T. Takahashi, Science and Technology of Ceramic Fuel Cells, Elsevier, Amsterdam, 1995.
[3] S.C. Singhal, K. Kendall, High-temperature Solid Oxide Fuel Cells: Fundamentals, Design and Applications, Elsevier, New York, 2003.
[4] N.Q. Minh, J. Am. Ceram. Soc. 76 (1993) 563–588.
[5] N.Q. Minh, Solid State Ion. 174 (2004) 271–277.
[6] P. Singh, N.Q. Minh, Int. J. Appl. Ceram. Technol. 1 (2004) 5–15.
[7] S.C. Singhal, Solid State Ion. 135 (2000) 305–313.
[8] S.C. Singhal, Solid State Ion. 152–153 (2002) 405–410.
[9] F. Tiez, Q. Fu, V. Haanappel, A. Mai, N.H. Menzler, S. Uhleenbruck, Int. J. Appl. Ceram. Technol. 4 (5) (2007) 436–445.
[10] L. Xue, E.A. Barringer, T. Cable, R. Goettler, K.E. Kniedel, Int. J. Appl. Ceram. Technol. 1 (1) (2004) 16–22.
[11] L. Xue, T. Cable, E.A. Barringer, Ceram. Eng. Sci. Proc. 24 (2003) 281–286.
[12] S. Elangovan, J.J. Hartvigssen, S.C. Kung, R.W. Goettler, E.A. Barringer, Proc. Electrochem. Soc. 2001-16 (2001) 94–99. (Solid Oxide Fuel Cell. VII).
[13] W. Schaefer, A. Koch, U. Herold-Schmidt, D. Stolten, Solid State Ion. 86–88 (1996) 1235–1239.
[14] M. Mogensen, K. Kammer, Annu. Rev. Mater. Res. 33 (2003) 321–331.
[15] S. McIntosh, R. Gorte, Chem. Rev. 104 (2004) 4845–4865.
[16] J. Wu, X. Yuan, J.J. Martin, H. Wang, J. Zhang, J. Shen, S. Wu, W. Merida, J. Power Sources 184 (2008) 104–119.
[17] S. Litster, G. McLean, J. Power Sources 130 (2004) 61–76.
[18] L.A. Shockling, P. Reichner, Proc. Electrochem. Soc. 89-14 (1989) 106–117.
[19] R.A. George, J. Power Sources 86 (2000) 134–139.
[20] S.E. Veyo, L.A. Shockling, J.T. Dederer, J.E. Gillett, W.L. Lundbery, J. Eng. Gas Turbines Power 124 (4) (2002) 845–849.
[21] W.L. Lundberg, S.E. Veyo, Proc. Electrochem. Soc. 2001-16 (2001) 78–87. (Solid Oxide Fuel Cell VII).
[22] W.L. Lundberg, S.E. Veyo, M.D. Moeckel, J. Eng. Gas Turbines Power 125 (1) (2003) 51–58.
[23] S. Alkaner, P. Zhou, J. Power Sources 158 (2006) 189–199.
[24] E. Antolini, Appl. Energy 8 (12) (2011) 4274–4293.
[25] R. George, N.F. Bessette, J. Power Sources 71 (1–2) (1998) 131–137.
[26] L. Lawlor, S. Griesser, G. Buchinger, A.G. Olabi, S. Cordiner, D. Meossner, J. Power Sources 193 (2) (2009) 387–399.
[27] K.S. Howe, G.J. Thompson, K. Kendall, J. Power Sources 196 (2011) 1677–1686.
[28] P. Sarkar, L. Yamarte, H. Rho, L. Johnson, Int. J. Appl. Ceram. Technol. 4 (2) (2007) 103–108.
[29] W.Z. Zhu, S.C. Deevi, Mater. Sci. Eng. A 348 (1–2) (2003) 227–243.
[30] J.W. Fergus, Mater. Sci. Eng. A 397 (1–2) (2005) 271–283.
[31] M.C. Tucker, J. Power Sources 195 (15) (2010) 4570–4582.
[32] N.P. Brandon, D. Corcoran, D. Cummins, A. Duckett, K. El-Khoury, D. Haigh, R. Leah, G. Lewis, N. Maynard, T. McColm, R. Trezona, A. Selcuk, M. Schmidt, J. Mater. Eng. Perform. 13 (2003) 253–256.
[33] C. Sun, R. Hui, J. Roller, J. Solid State Electrochem. 14 (2010) 1125–1144.
[34] S. Skinner, Int. J. Inorg. Mater. 3 (2) (2001) 113–121.
[35] H. Yokogawa, T. Horita, N. Sakai, K. Yamaji, M.E. Brito, Y.P. Xiong, H. Kishimoto, Solid State Ion. 177 (35–36) (2006) 3193–3198.
[36] M. Kornely, A. Neumann, N.H. Menzler, A. Weber, E. Ivers-Tiffee, ECS Trans. 35 (2011) 2009–2017.
[37] K. Tomida, A. Yamashita, H. Tsukuda, T. Kabata, K. Ikeda, N. Hisatome, Y. Yamazaki, Electrochemistry 77 (12) (2009) 1018–1027.
[38] T. Ohrn, Z. Liu, in: Proc. 12th SECA Workshop, Pittsburgh (July 2011).
[39] T. Ujii, ECS Trans. 7 (1) (2007) 3–9.
[40] L. Blum, W.A. Meulenberg, H. Nabielek, R. Steinberg-Wilckens, Int. J. Appl. Ceram. Technol. 2 (6) (2005) 482–492.
[41] R.M. Ormerod, Chem. Soc. Rev. 32 (2003) 17–28.
[42] A.B. Stambouli, E. Traversa, Renew. Sustain. Energy Rev. 6 (5) (2002) 433–455.
[43] D.J.L. Brett, A. Atkinson, N.P. Brandon, S. Skinner, Chem. Soc. Rev. 37 (2008) 1568–1578.
[44] O. Yamamoto, Electrochem. Acta 45 (15–16) (2000) 2423–2435.
[45] S.C. Singhal, in: T. Seiyama (Ed.), Proceedings Fukuoka International Symposium on Global Environment and Energy Issues, The Electrochemical Society of Japan, 1990, pp. 95–104.
[46] S.C. Singhal, in: F. Grosz (Ed.), Proceedings Second International Symposium on Solid Oxide Fuel Cells, Commission of the European Communities, Luxembourg, 1991, pp. 25–33.
[47] S.C. Singhal, in: Proceedings of the International Forum on Fine Ceramics, Japan Fine Ceramics Center, Nagoya, Japan, 1992, pp. 159–167.
[48] S.C. Singhal, in: S.P.S. Badwal (Ed.), Proceedings of the Fifth International Conference on the Science and Technology of Zirconia, Technomic Publishing Company, Lancaster, PA, 1993, pp. 631–651.
[49] S.C. Singhal, in: S.C. Singhal, H. Iwahara (Eds.), Proceedings of the Third International Symposium on Solid Oxide Fuel Cells, The Electrochemical Society, Pennington, NJ, 1993, pp. 665–677.
[50] S.C. Singhal, in: M. Dokiya (Ed.), Proceedings of the Fourth International Symposium on Solid Oxide Fuel Cells, The Electrochemical Society, Pennington, NJ, 1995, pp. 195–207.
[51] S.C. Singhal, in: F.W. Poulson, N. Bonanos, S. Linderoth, M. Mogensen, B. Zachau-Christiansen (Eds.), Proceedings of the 17th Risø International Symposium on Materials Science: High Temperature Electrochemistry – Ceramics and Metals, Risø National Laboratory, Roskilde, Denmark, 1996, pp. 123–138.
[52] S.C. Singhal, in: U. Stimming (Ed.), Proceedings of the Fifth International Symposium on Solid Oxide Fuel Cells, The Electrochemical Society, Pennington, NJ, 1997, pp. 37–50.
[53] S.C. Singhal, in: Dan A. Dolenc (Ed.), Proceedings of the 1998 International Gas Research Conference, Gas Research Institute, Chicago, IL, 1998, pp. 822–833.
[54] S.C. Singhal, in: P. Vincenzini (Ed.), Proceedings of the World Ceramics Congress and Forum on New Materials, Techna Srl, Italy, 1999.
[55] S.C. Singhal, S. Gopalan, in: P. Kumta, A. Manthiram (Eds.), Processing and Characterization of Electrochemical Materials and Devices, The American Ceramic Society, Inc., Westerville, OH, 1999.
[56] S.C. Singhal, in: S.C. Singhal, M. Dokiya (Eds.), Proceedings of the Sixth International Symposium on Solid Oxide Fuel Cells, The Electrochemical Society, Pennington, NJ, 1999, pp. 39–51.
[57] S.C. Singhal, Mater. Res. Soc. Bull. 25 (2000) 16–21.
[58] H. Möbius, J. Solid State Electrochem. 1 (1997) 2–16.
[59] S.E. Veyo, A. Kusunoki, S. Takeuchi, S. Kaneko, H. Yokoyama, Proc. Am. Power Conf. 56 (1) (1994) 159–165.
[60] A. Iyengar, N. Desai, S. Vora, L.A. Shockling, J. Fuel Cell Sci. Technol. 7 (6) (2010) 061002–061008.
[61] S. Vora, in: Proc. 10th SECA Workshop, Pittsburgh (July 2009).
[62] S. Vora, in: Proc. 9th SECA Workshop, Pittsburgh (July 2008).
[63] K. Huang, 7th European Solid Oxide Fuel Cell Forum, Lucerne, P0303, Switzerland, 3–7 July 2006.
[64] U.B. Pal, S.C. Singhal, High Temp. Sci. 27 (1990) 251–264.
[65] U.B. Pal, S.C. Singhal, J. Electrochem. Soc. 137 (1990) 2937–2941.
[66] A.O. Isenberg, in: J.D.E. McIntyre (Ed.), Proc. Sym. Electrode Materials, Processes for Energy Conversion and Storage, The Electrochemical Society, New Jersey, 1977, pp. 572–583.
[67] O. Kesler, Mater. Sci. Forum 539–543 (Pt. 2) (2007) 1385–1390. (THERMEC 2006).
[68] K. Huang, H.D. Harter, Solid State Ion. 181 (2010) 941–946.
[69] A. Kawakami, S. Matsuoka, N. Watanabe, T. Saito, A. Ueno, T. Ishihara, N. Sakai, H. Yokokawa, Ceram. Eng. Sci. Proc. 27 (4) (2007) 3–13. (Advances in Solid Oxide Fuel Cells II).
[70] H.U. Anderson, F. Tietz, Interconnect, in: S.C. Singhal, K. Kendall (Eds.), High Temperature Solid Oxide Fuel Cells: Fundamentals, Design and Applications, Elsevier, Oxford, UK, 2003, p. 179. (Chapter 7).
[71] L.A. Chick, J. Liu, J.W. Stevenson, T.R. Armstrong, D.E. McCready, G.D. Maupin, G.W. Coffey, C.A. Coyle, J. Am. Ceram. Soc. 80 (8) (1997) 2109–2120.
[72] L.J.H. Kuo, S.D. Vora, S.C. Singhal, J. Am. Ceram. Soc. 80 (1997) 589–593.
[73] K. Huang, ECS Trans. 12 (2007) 375–383.
[74] G. Digiuseppe, R. Drapper, J. Fuel Cell Sci. Technol. 5 (2) (2008) 021013–021019.
[75] S. Gopalan, G. DiGiuseppe, J. Power Sources 125 (2) (2004) 183–188.
[76] N.J. Maskalick, Proc. Electrochem. Soc. 89-11 (1989) 279–287.
[77] R.A. George, Proc. Am. Power Conf. 59 (1) (1997) 548–550.
[78] N.F. Bessette, R.A. George, Denki Kagaku oyobi Kogyo Butsuri Kagaku 64 (6) (1996) 602–608.
[79] L.A. Shockling, J.M. Makiel, in: Proc. Intersoc. Ener. Conv. Eng. Conf., 25th 1990, pp. 224–229.
[80] S.E. Veyo, in: Proc. Intersoc. Ener. Conv. Eng. Conf., 31st 1996, pp. 1138–1143.
[81] M.H. Yokoyama, S.E. Veyo, Proc. Electrochem. Soc. 97-40 (1997) 94–103.
[82] W.L. Lundbergh, L.A. Shockling, S.E. Veyo, E. Smelzer, G. Israelson, A. Iyengar, in: Proc. Ann. Intl. Pitt. Coal Conf., 25th 2008, pp. 42/1–42/14.